The regulation of coralline algal physiology, an *in-situ* study of *Corallina officinalis* (Corallinales, Rhodophyta)

Williamson Christopher James[1,2*], Perkins Rupert[3], Voller Matthew[1], Yallop Marian Louise[2], Brodie Juliet[1].

1. The Natural History Museum, Department of Life Sciences, Cromwell Road, London SW7 5BD, UK
2. School of Biological Sciences, Life Sciences Building, 24 Tyndall Avenue, Bristol, BS8 1TQ, UK
3. School of Earth and Ocean Sciences, Cardiff University, Cardiff, CF10 3AT, UK

*Corresponding author Email: c.williamson@nhm.ac.uk

Running title: Drivers of coralline algae physiology

Keywords: *Corallina*, calcification, productivity, respiration, carbonate chemistry, ocean acidification, climate change

Abstract

Calcified macroalgae are critical components of marine ecosystems worldwide, but face considerable threat both from climate change (increasing water temperatures) and ocean acidification (decreasing ocean pH and carbonate saturation). It is thus fundamental to constrain the relationships between key abiotic stressors and the physiological processes that govern coralline algal growth and survival. Here we characterize the complex relationships between the abiotic environment of rock pool habitats, and the physiology of the geniculate red coralline alga, *Corallina officinalis* (Corallinales, Rhodophyta). Paired assessment of irradiance, water temperature and carbonate chemistry, with *C. officinalis* net production (*NP*), respiration (*R*) and net calcification (*NG*) was performed in a south-west UK field site, at multiple temporal scales (seasonal, diurnal and tidal). Strong seasonality was observed in *NP* and night-time *R*, with a P_{max} of 22.35 μmol DIC gDW^{-1} h^{-1}, E_k of 300 μmol photons m^{-2} s^{-1} and *R* of 3.29 μmol DIC gDW^{-1} h^{-1} determined across the complete annual cycle. *NP* showed a significant exponential relationship with irradiance ($R^2 = 0.67$), although was temperature dependent given ambient irradiance > E_k for the majority of the annual cycle. Over tidal emersion periods, dynamics in *NP* highlighted the ability of *C. officinalis* to acquire inorganic carbon despite significant fluctuations in carbonate chemistry. Across all data, *NG* was highly predictable ($R^2 = 0.80$) by irradiance, water temperature and carbonate chemistry, providing a NG_{max} of 3.94 μmol $CaCO_3$ gDW^{-1} h^{-1}, and E_k of 113 μmol photons m^{-2} s^{-1}. Light-*NG* showed strong seasonality and significant coupling to *NP* ($R^2 = 0.65$), as opposed to rock pool water carbonate saturation. In contrast, the direction of dark-*NG* (dissolution vs. precipitation) was strongly related to carbonate saturation, mimicking abiotic precipitation dynamics.

Data demonstrated that *C. officinalis* is adapted to both long-term (seasonal) and short-term (tidal) variability in environmental stressors, although the balance between metabolic processes and the external environment may be significantly impacted by future climate change.

1. Introduction

Calcified macroalgae are critical components of marine ecosystems from polar to tropical regions (Littler et al., 1985, McCoy and Kamenos, 2015), constituting one of the most important structural elements in many coastal zones (van der Heijden and Kamenos, 2015). In shallow temperate areas, heavily calcified 'coralline' red macroalgae (Corallinales, Rhodophyta) act as autogenic ecosystem engineers (Johansen, 1981; Jones et al., 1994; Nelson, 2009), providing habitat for numerous small invertebrates, shelter from the stresses of intertidal life via their physical structure, and surfaces for the settlement of epifauna and microalgal epiphytes (Nelson, 2009; Perkins et al., 2016). Temperate corallines are also of significant importance in the carbon and carbonate cycles of shallow coastal ecosystems, due to their relatively high productivity and calcium carbonate precipitation and dissolution (Martin and Gattuso, 2009; van der Heijden and Kamenos, 2015).

Species of the geniculate (jointed) coralline genus *Corallina* form extensive turfs across large areas of NE Atlantic intertidal regions, providing substratum, habitat and refugia for a number of important organisms (Coull and Wells, 1983; Kelaher, 2002; 2003; Hofmann et al., 2012a; Brodie et al., 2016; Perkins et al., 2016). Within rock pool habitats, *Corallina* must maintain productivity and growth under the influence of a myriad of highly variable stressors, including irradiance, water temperature and

carbonate chemistry, which fluctuate on seasonal, diurnal and tidal time scales (Egilsdottir et al., 2013; Williamson et al., 2014a). During summer, high irradiance, water temperature, pH and carbonate saturation (ΩCO_3^{2-}) dominate, whilst winter is associated with limiting irradiance and temperature, and decreased water pH (i.e. increased acidity) and ΩCO_3^{2-} (Ganning, 1971; Morris and Taylor, 1983; Williamson et al., 2014a). Across daytime tidal emersion periods, rock pool water temperatures generally increase and community photosynthetic activity serves to strip CO_2 and HCO_3^- from the water, with concomitant increases in pH and ΩCO_3^{2-} (Williamson et al., 2014a). In contrast, night-time emersion is dominated by respiration processes within rock pools, with CO_2 production driving down water pH and ΩCO_3^{2-} (Morris and Taylor, 1983). In order to sustain their dominance of temperate coastlines, *Corallina* must balance this environmental variability with their requirements for key physiological processes, including photosynthesis, respiration and calcification.

The interactions between *Corallina* physiology and environmental variability are likely to be significantly impacted by on-going climate change (increasing temperatures) and ocean acidification (decreasing pH and ΩCO_3^{2-}) (Hofmann et al., 2012a;b; McCoy and Kamenos, 2015). Water temperature profoundly influences the survival, recruitment, growth and reproduction of macroalgal species (Breeman, 1988), and is a key factor governing both the small- and large-scale distribution of species (Breeman, 1988; Luning, 1990; Jueterbock et al., 2013). With continued increases in water temperatures, some macroalgal species and populations may become chronically (gradual warming) or acutely (extreme events) stressed as temperatures exceed physiological thresholds (Brodie et al., 2014). With OA driven increases in seawater dissolved organic carbon (DIC) concentrations, several studies have predicted a positive response of macroalgal

photosynthesis (Marberly, 1990; Johnston et al., 1992), though with notable exceptions (Israel and Hophy, 2002). Such responses are likely to be determined by the ability of macroalgae to utilize seawater HCO_3^-, and whether photosynthesis is saturated at current seawater DIC (Koch et al., 2013). In contrast, calcification and dissolution processes of calcified macroalgae are likely to be negatively impacted by OA driven changes in seawater carbonate chemistry (Ries, 2011; Koch et al., 2013). In particular, increases in CO_2 and H^+ in external seawater will increase diffusion rates to internal sites of calcification, lowering internal ΩCO_3^{2-}, and decreasing $CaCO_3$ precipitation (Jokiel, 2011; Ries, 2011; Koch et al., 2013). The ability to control ion transport across membranes and internal pH regulation, are therefore likely to be major factors determining calcified macroalgal responses to OA (Koch et al., 2013). It is therefore critical to constrain *Corallina* ecophysiology in relation to current environmental variability, to aid projections under future climate scenarios (Nelson, 2009; Koch et al., 2013; Brodie et al., 2014; Hofmann and Bischof, 2014). It is also important to understand the present-day role of these dominant community members in coastal carbon cycles and how this may change into the future (van der Heijden and Kamenos, 2015).

This study focuses on *Corallina officinalis*, a species that dominates North Atlantic turfing assemblages (Williamson et al., 2015) and has been the focus of recent studies aiming to understand coralline algal physiology and future fate (Hofmann et al., 2012a,b; Williamson et al., 2014a,b; Williamson et al., 2015; Perkins et al., 2016). Whilst the skeletal mineralogy (Williamson et al., 2014b), photophysiology (Williamson et al., 2014a; Perkins et al., 2016), and phylogenetics of *C. officinalis* (Williamson et al., 2015) have been examined, information on *in-situ* physiology in

relation to key environmental stressors is currently lacking. We therefore performed the first high-resolution *in-situ* assessment of *C. officinalis* physiology (production, respiration and calcification) in relation to key environment stressors (irradiance, temperature and carbonate chemistry) over both daytime and night-time tidal emersion periods, across multiple seasons. By characterizing the influence of abiotic stressors on key physiological processes, this study advances efforts to understand the ecology and fate of coralline algae in a changing world.

2. Methods

This study was conducted at Combe Martin (CM), north Devon, UK (51^{o}12'13N 4^{o}2'19W, Fig. 1), a north-west facing rocky intertidal site, positioned within a sheltered bay. *Corallina officinalis* dominates intertidal rock pools at CM, including large (ca. 40 m^3, 0.5 m depth) upper shore (Chart Datum + 5.5 m) rock pools created by a man-made walkway (Fig. 1b and 1c). This site is located in the middle of *C. officinalis'* range across the NE Atlantic, which spans from Iceland to northern Spain (Williamson et al., 2015).

To assess *C. officinalis* net production, respiration and calcification, incubation experiments were performed at CM during daytime tidal emersion in December 2013, and March, July and September 2014, and night-time tidal emersion during the latter three sampling months (sampling dates and tidal timings are presented in Table 1), to capture the tidal, diurnal and full seasonal dynamics in physiology. Two sets of approximately 1 h timed incubations were performed per emersion period, at both the start (initiated within 30 mins of tidal emersion) and end (over the final 1.5 h) of

emersion. Irradiance and rock pool water salinity, temperature and carbonate chemistry were monitored in parallel throughout.

2.1. Physiology incubations

Net production (*NP*) and respiration (*R*) (DIC flux, μmol g dry weight $(DW)^{-1}$ h^{-1}), and net light and dark calcification rates (*NG*) (μmol $CaCO_3$ gDW^{-1} h^{-1}) were determined using closed chamber incubations. Ten discrete *C. officinalis* fronds were collected randomly across upper shore CM rock pools of the same shore height, and similar size/depth, and placed individually into 0.5 l clear glass chambers filled with rock pool water. Our previous study in these upper shore rock pools revealed no significant difference in the progression of temperature or carbonate chemistry dynamics over summer or winter tidal emersion periods (Williamson et al. 2014). Final dry weight of incubated *C. officinalis* averaged 4.0 ± 0.15 g across incubations. Two additional chambers were filled only with rock pool water to serve as controls for non-*Corallina* biological activity. At the beginning of incubations, 100 ml initial rock pool water samples were collected for pH and total alkalinity (TA) determination (see below), and poisoned with saturated mercuric chloride solution to prevent biological activity. Incubation chambers were then sealed, and six chambers (5 *Corallina*, 1 control) positioned in an upper shore rock pool to maintain ambient irradiance and temperature conditions (both during day and night-time). The remaining six chambers (5 *Corallina*, 1 control) were placed in opaque bags to create dark conditions during daytime incubations (or shield from moonlight during night-time) and placed within the same rock pool to maintain ambient temperature. After incubating for ca. 1 h, chambers were removed from the rock pool and a final 100 ml water sample was collected from each chamber for pH and TA measurements. In parallel to all incubations, ambient irradiance

(PAR μmol photons m^{-2} s^{-1}), rock pool water temperature (°C), and salinity (S), were monitored every 30 min using a 2-pi LI-COR cosine-corrected quantum sensor positioned ca. 5 cm above the surface of the rock pool (15 s average irradiance measurements were taken using an in-built function of the sensor), a digital thermometer, and a hand-held refractometer, respectively. Cumulative photodose (PAR, mol photons m^{-2}) was calculated from irradiance measurements by integrating PAR over time from the start of tidal emersion of rock pools. Following incubations, *C. officinalis* fronds were collected from incubation chambers for weighing after drying at 100°C for 24 h.

The pH (total scale) of water samples was measured immediately using a Mettler Toledo Inlab-expertpro pH probe calibrated using Tris-buffers (pH 4, 7, and 10) prepared in artificial seawater. TA of water samples was measured by the potentiometric method using Gran titration with a Mettler Toledo DL50 Graphix automatic titrator. Reference material measurements of Na_2CO_3 standards (0.5 and 1 mmol kg^{-1}) prepared in 0.6 mol kg^{-1} NaCl background medium were used to correct sample measurement for accuracy. The relative error of TA measurements was 4.6 ± 0.24 %, with a relative standard deviation of 3.35 ± 1.5 %. pH, TA, water temperature and salinity were subsequently input into CO2SYS v2.1 (Pierrot et al., 2016) to determine all carbonate chemistry parameters (DIC, pCO_2, HCO_3^-, CO_3^{2-} and the saturation states of aragonite [Ω_{arg}] and calcite [Ω_{cal}]), allowing both calculation of *C. officinalis NP/R* (ΔDIC) and *NG* (ΔTA) during incubations, and the monitoring of ambient rock pool water carbonate chemistry. CO2SYS was run using the constants of Mehrbach et al. (1973) refitted by Dickson and Millero (1987). The carbonate chemistry of rock pool water was represented by initial water samples (n = 12) collected

at the beginning of each incubation experiment, providing an assessment of water chemistry at both the start and end of tidal emersion periods, matching productivity analyses. *C. officinalis NP* (assessed from daytime light treatment incubations) and *R* (assessed from daytime dark treatment and all night-time incubations) were calculated from the difference between initial and final incubation DIC concentrations, as:

$$NP\ or\ R_{DAY/NIGHT} = \left(\frac{\Delta DIC\ v}{dw\ \Delta t}\right) - NG$$

where *NP* and $R_{DAY/NIGHT}$ are net production and respiration during the day or night, respectively (μmol DIC gDW^{-1} h^{-1}); ΔDIC is the change in dissolved inorganic carbon concentration during the incubation (μmol DIC kg^{-1} seawater); v is the incubation chamber volume (l); dw is the dry weight of *C. officinalis* incubated (g); Δt is the incubation time (h); and *NG* is the net calcification rate (μmol $CaCO_3$ gDW^{-1} h^{-1}). *NG* was estimated using the alkalinity anomaly technique (Smith and Key, 1975; Chisholm and Gattuuso, 1991), whereby TA decreases by 2 equivalents for each mol of $CaCO_3$ precipitated. Light calcification (assessed from daytime light treatment incubations) and dark calcification (assessed from daytime dark and all night-time incubations) were thus calculated as:

$$NG_{DAY}(or\ NG_{NIGHT})_{-LIGHT/DARK} = \frac{\Delta TA\ v}{2(dw\ \Delta t)}$$

where $NG_{DAY\text{-}LIGHT/DARK}$ *and* $NG_{NIGHT\text{-}LIGHT/DARK}$ are net calcification during daytime or night-time tidal emersion periods, determined from light or dark treatment incubations (μmol $CaCO_3$ gDW^{-1} h^{-1}); ΔTA is the change in total alkalinity during the incubation

(μmol kg^{-1} seawater); v is the incubation chamber volume (l); dw is the dry weight of *C. officinalis* incubated (g); and Δt is the incubation time (h).

2.2. Data analysis

All statistical analyses and plotting of data were performed using R v.3.0.2 (R Core Team, 2014). Prior to all analyses, normality of data was tested using the Shapiro-Wilk test and examination of frequency histograms. If data were not normally distributed, Box-Cox power transformation was applied using the boxcox function of the MASS package (Venables and Ripley, 2002), and normality re-checked. Following the application of models to data, model assumptions were checked by examination of model criticism plots. Whilst sampling for determination of *NP*, *R* and *NG* was performed in the same rock pools over a number of dates at each site, measurements were performed on different individuals during each sampling date and thus repeated measures analysis of variance (ANOVA) was not utilized during the present study.

Abiotic Environment: Differences in irradiance and rock pool water temperature between sampling months and tidal emersion periods were examined using 2-way ANOVA with interaction. Post hoc Tukey honest significant differences analysis was performed on all significant ANOVA results. To facilitate comparison of rock pool water carbonate chemistry between months and tidal emersion periods, all variables were summarized using principal components analysis (PCA) with scaled variables, allowing for transformation of the highly correlated carbonate chemistry variables into uncorrelated PCs for comparison between independent variables (month and tide). Differences in carbonate chemistry were thus examined by ANOVA analysis of principal component one (PC1) separately for daytime and night-time data, as above.

Least squares multiple linear regression was used to examine relationships between daytime PC1 and irradiance (analysed separately as both irradiance measured and calculated cumulative photodose) and rock pool water temperature. The relative importance of predictor variables was calculated using the relaimpo package with type 'lmg' (Grömping, 2006). Least squares linear regression was used to examine relationships between night-time PC1 and rock pool water temperature.

Net production, respiration and calcification: NP, $R_{DAY/NIGHT}$ and *NG* rates were analyzed separately for daytime and night-time data using 3-way ANOVA with the factors month, tide and light-treatment, with all interactions. All *C. officinalis NP/R* and *NG* data measured across all seasons were plotted as an exponential function *P-E* of the average ambient irradiance *E* (µmol photons m^{-2} s^{-1}) recorded over each incubation experiment, as:

$$NP/R\ (NG) = P_{max}\left(1 - e^{-E/Ek}\right) + c$$

where P_{max} is the rate of maximum net production (or calcification) (µmol DIC gDW^{-1} h^{-1}, or µmol $CaCO_3$ gDW^{-1} h^{-1}); E_k is the minimum saturating irradiance (µmol m^{-2} s^{-1}); and *c* is the dark respiration rate (or calcification rate) (µmol DIC/$CaCO_3$ gDW^{-1} h^{-1}). To examine relationships between *NP, R* and *NG* with water temperature and carbonate chemistry ($PC1_{day/night}$), temperature and PC1 were added individually into the above model as linear terms, in addition to construction of a 'global model' containing irradiance as an exponential function, and both water temperature and PC1 as linear terms. The goodness-of-fit of the respective models was compared using estimated R^2 and Akaike Information Criterion (AIC), and ANOVA comparisons were performed to

test the significance of the inclusion of respective terms into each model. The relationship between *C. officinalis NG* and *NP/R* was modeled using non-linear regression as detailed above.

3. Results

3.1. Abiotic environment

Irradiance varied between all sampling months ($F_{3,32}$ = 193.385, P < 0.0001), being maximal in July and minimal in December (Fig. 2), with significant change in irradiance over tidal emersion only apparent in July ($F_{1,32}$ = 8.114, P < 0.01, TukeyHSD P < 0.05). Warmest daytime rock pool water temperatures were observed in July, with the coldest in March, and a significant difference apparent between all sampling months ($F_{3,32}$ = 760.94, P < 0.0001) (Fig. 2). Water temperature significantly increased over daytime tidal emersion during July and September ($F_{1,32}$ = 97.48, P < 0.0001, TukeyHSD P < 0.05 in both cases), whereas no change occurred in December or March, as supported by significant interaction between month and tide ($F_{3,32}$ = 37.01, P < 0.0001). Night-time rock pool water temperatures were greatest in September and lowest in March, with a significant difference between all sampling months ($F_{2,13}$ = 168.534, P < 0.0001). Over night-time tidal emersion, a significant decrease in water temperature was apparent during July (15.6 ± 0.16 to 14.7 ± 0.14^{o}C) and September (16.8 ± 0.45 to 15.7 ± 0.15^{o}C) ($F_{1,13}$ = 20.049, P < 0.01, TukeyHSD P < 0.05 in all cases).

Changes in rock pool water carbonate chemistry were observed over daytime and night-time tidal emersion periods during each sampling month (Supplementary Figures 1 & 2). Over daytime emersion, pCO_2 and HCO_3^- decreased, with concomitant increases in

pH, CO_3^{2-}, Ω_{arg} and Ω_{cal}. From the start to end of night-time emersion, the opposite trends were observed, with increases in pCO_2 and HCO_3^- paralleled by decreases in pH and ΩCO_3^{2-}. Principal components analysis (PCA) served to summarize daytime and night-time carbonate chemistry parameters for subsequent analyses (Table 2 & Fig. 3), with $PC1_{day}$ and $PC1_{night}$ describing 84 % and 83 % of the variance in carbonate chemistry observed over seasonal and tidal time-scales, respectively. For all subsequent analyses, $PC1_{day}$ and $PC1_{night}$ were taken as representative of carbonate chemistry dynamics.

$PC1_{day}$ and $PC1_{night}$ were significantly different between sampling months ($F_{3,67}$ = 27.528 and $F_{2,47}$ = 39.73, respectively, $P < 0.0001$ in both cases, Fig. 4), with higher $PC1_{day}$ observed in July and September in comparison to December and March, and significantly different $PC1_{night}$ observed between all night-time sampling months (March, July and September; TukeyHSD, $P < 0.05$ in all cases). $PC1_{day}$ significantly increased over daytime tidal emersion, representing decreased DIC, pCO_2 and HCO_3^-, and increased pH and ΩCO_3^{2-} parameters, during all sampling months but December ($F_{1,67}$ = 1.912, $P < 0.0001$, TukeyHSD $P < 0.05$ in all cases). Over night-time tidal emersion the opposite trends were observed, with significant decrease in $PC1_{night}$ apparent during every sampling month, representing increased DIC, pCO_2 and HCO_3^- and consequent decreases in pH and ΩCO_3^{2-} ($F_{1,47}$ = 810.90, $P < 0.0001$, TukeyHSD $P < 0.05$ in all cases). The magnitude of change in rock pool water carbonate chemistry over night-time tidal emersion increased from March to September, as evidenced by significant interaction between month and tide ($F_{2,47}$ = 73.31, $P < 0.0001$).

Least squares multiple linear regression (Table 3) revealed significant relationships between $PC1_{day}$, irradiance (28% relative importance) and water temperature (71% relative importance) ($R^2 = 0.63$, $P < 0.0001$) (Table 3), and between $PC1_{day}$, calculated cumulative photodose (58% relative importance) and water temperature (41% relative importance) ($R^2 = 0.69$, $P < 0.0001$). $PC1_{night}$ showed a minimal relationship to water temperature ($R^2 = 0.08$, $P < 0.05$).

3.2. Net production and respiration

Corallina officinalis demonstrated maximal *NP* (negative DIC flux) in July (start of emersion = 25.80 ± 0.94 μmol DIC gDW^{-1} h^{-1}), with lowest values recorded during December and March (end of March emersion = 1.56 ± 0.74 μmol DIC gDW^{-1} h^{-1}) ($F_{3,69} = 6.838$, $P < 0.001$) (Fig. 5). In contrast, no significant difference in *C. officinalis* R_{DAY} was observed between sampling months (Fig. 5a). Whilst significant changes in *NP* and R_{DAY} were recorded in relation to the factor tide ($F_{1,69} = 8.684$, $P < 0.01$), post-hoc TukeyHSD did not recover significant differences in either parameter between the start and end of tidal emersion, within any sampling month. Over night-time tidal emersion, no significant difference was apparent in R_{NIGHT} between light treatment or the start and end of tidal emersion periods, and thus data are pooled for presentation (Fig. 6a). Across sampling months, a significant increase in *C. officinalis* R_{NIGHT} was apparent from March to July and September ($F_{2,52} = 22.170$, $P < 0.0001$), with ca. 4.5-fold greater R_{NIGHT} observed during September as compared to March.

Across all data, *NP* showed a significant relationship with irradiance ($R^2 = 0.67$, $P < 0.0001$ for all parameters, AIC = 885.64), giving a P_{max} of 22.35 μmol DIC gDW^{-1} h^{-1}, E_k of 301 μmol photons m^{-2} s^{-1} and estimated overall respiration rate of 3.29 μmol DIC

347 gDW^{-1} h^{-1} (Fig. 7a, Table 4). Addition of water temperature and carbonate chemistry
348 (both individually and together) into the model did not significantly improve the
349 goodness-of-fit (Table 4). This may be due to correlations between irradiance and water
350 temperature (r = 0.42, $P < 0.0001$), irradiance and PC1 (r = 0.19, $P < 0.05$) and
351 temperature and PC1 (r = 0.59, $P < 0.0001$) (data not shown).
352
353 **3.3. Calcification**
354 *Corallina officinalis* NG_{DAY} was greatest during July and September as compared to
355 December and March ($F_{3,69} = 16.814$, $P < 0.0001$, TukeyHSD $P < 0.05$ in all cases),
356 with a significant difference between $NG_{DAY\text{-}LIGHT}$ and $NG_{DAY\text{-}DARK}$ apparent in all
357 sampling months ($F_{1,69} = 290.075$, $P < 0.0001$) (Fig. 5b). Highest $NG_{DAY\text{-}LIGHT}$ (4.62 ±
358 0.45 μmol $CaCO_3$ gDW^{-1} h^{-1}) was recorded at the end of daytime tidal emersion during
359 July, with lowest $NG_{DAY\text{-}LIGHT}$ (1.70 ± 0.08 μmol $CaCO_3$ gDW^{-1} h^{-1}) recorded at the end
360 of tidal emersion during December. Both negative (indicating $CaCO_3$ dissolution) and
361 positive (indicating $CaCO_3$ precipitation) $NG_{DAY\text{-}DARK}$ values were observed, with
362 maximal $CaCO_3$ dissolution in the dark (-0.53 ± 0.20 μmol $CaCO_3$ gDW^{-1} h^{-1}) at the
363 start of March daytime tidal emersion and maximal precipitation in the dark (2.01 ±
364 0.35 μmol $CaCO_3$ gDW^{-1} h^{-1}) at the end of September daytime tidal emersion (Figure
365 5b). Significant differences in NG_{DAY} observed in relation to tide ($F_{1,69} = 5.028$, $P <$
366 0.05) were confined to increases in $NG_{DAY\text{-}DARK}$ from the start to end of July and
367 September tidal emersion periods (TukeyHSD $P < 0.05$ in both cases), with significant
368 interaction between month and tide ($F_{3,69} = 5.104$, $P < 0.01$). No significant differences
369 in $NG_{DAY\text{-}LIGHT}$ were observed between the start and end of tidal emersion periods
370 despite concomitant increases in rock pool water ΩCO_3^{2-}.
371

During night-time tidal emersion, there was no significant difference between $NG_{NIGHT\text{-}LIGHT}$ and $NG_{NIGHT\text{-}DARK}$, or between the start and end of tidal emersion within any sampling month, and thus data are pooled for presentation (Fig. 6b). Whilst net $CaCO_3$ dissolution was observed during both March and September night-time tidal emersion, with maximal dissolution in the latter month (monthly average of -0.83 ± 0.11 μmol $CaCO_3$ gDW^{-1} h^{-1}), net $CaCO_3$ precipitation was apparent across the duration of July night-time emersion (monthly average of 0.46 ± 0.14 μmol $CaCO_3$ gDW^{-1} h^{-1}); rates being significantly different between all sampling months ($F_{2,52}$ = 25.50, P < 0.0001, TukeyHSD P < 0.05 in all cases) (Fig. 6b).

Across all data, *NG* showed a significant exponential relationship with ambient irradiance (estimated R^2 = 0.76, P < 0.0001 for all parameters, AIC = 383.17), providing a NG_{max} of 4.41 μmol $CaCO_3$ gDW^{-1} h^{-1}, and an E_k of 201 μmol photons m^{-2} s^{-1} (Fig. 7b, Table 4). Addition of water temperature and/or carbonate chemistry (as PC1) increased the goodness-of-fit (estimated R^2 and AIC) of the models to *NG* data (Table 4). The best representation of *NG* was provided by the 'global model' including irradiance as exponential term, and both water temperature and carbonate chemistry as linear terms (estimated R^2 = 0.80, P < 0.05 for all parameters, AIC = 360.57), providing a NG_{max} of 3.94 μmol $CaCO_3$ gDW^{-1} h^{-1}, and an E_k of 113 μmol photons m^{-2} s^{-1} (Table 4). ANOVA comparison demonstrated all *NG* models to be significantly different to one another (data not shown). Across all data, a significant relationship was also identified between *NG* and *NP/R* (R^2 = 0.65, P < 0.05 for all parameters, n = 140) (Fig. 8).

4. Discussion

Through the pairing of physiological and environmental monitoring, this study has constrained the regulation of key physiological processes of a coralline alga by irradiance, water temperature and carbonate chemistry. It is fundamental to understand the interactions of coralline algae with their environment, given the continuing perturbation of key abiotic stressors by climate change and ocean acidification. The findings presented here are discussed in regards to the ecophysiology of *Corallina officinalis* and coralline algae in general, within the larger perspective of global change.

4.1. Production and respiration

This study highlights significant seasonality in *C. officinalis* net production that follows dynamics in irradiance, water temperature and carbonate chemistry. In marine macrophytes, photosynthetic capacity is generally greatest during months when irradiance and temperature are highest (Lüning, 1990; Cabello-Pasini and Alberte, 1997). Consistent with previous accounts for other calcifying macroalgae (e.g. Martin et al., 2006; 2007; Egilsdottir et al., 2015), *C. officinalis* net production was maximal during July and minimal in December, showing a significant exponential relationship with irradiance ($R^2 = 0.67$). At saturating levels of irradiance, the enzymatic reactions that limit photosynthesis are, however, temperature dependent (Lüning, 1990). The light-saturation coefficient (E_k) determined by the present study (ca. 300 μmol photons m^{-2} s^{-1} ambient irradiance) highlighted that *C. officinalis* photosynthesis was light-saturated for the majority of the annual cycle; ambient irradiance > E_k was recorded in every sampling month other than December, consistent with the findings of Williamson et al. (2014a). Thus maximal rates of *C. officinalis* production were likely temperature-dependent, as is known for other intertidal macroalgae (Kanwisher, 1966).

Strong seasonality was also identified in *C. officinalis* dark respiration determined during night-time incubations, in line with accounts for other coralline algae (e.g. Martin et al., 2006; Egilsdottir et al., 2015). The ca. 4.5-fold increase observed in night-time respiration from March to September is within the range reported for the maerl-forming species, *Lithothamnion coralloides*, which demonstrated a 3-fold increase in respiration during summer months (Martin et al., 2006), and the closely related geniculate species, *Ellisolandia elongata*, which demonstrated a 10-fold summer increase in respiration (Egilsdottir et al., 2015). Whilst night-time respiration rates determined here for *C. officinalis* (ca 1 – 4.5 μmol DIC gDW^{-1} h^{-1}) fall within the lower end of the range reported for *E. elongata* from similar habitats (ca. 0.4 - 17 μmol CO_2 gDW^{-1} h^{-1}), Egilsdottir et al. (2015) note that their high summer rates were likely driven by high water temperatures during summer measurements (23ºC as compared to 16ºC during the present study).

Consistent with observations made in *E. elongata* dominated habitats (Bensoussan and Gattuso, 2007), *C. officinalis* demonstrated increased rates of daytime respiration as compared to night-time, with 6-fold greater daytime rates during March, and 1.1-times greater rates during July and September. Previously, Bensoussan and Gattuso (2007) observed large variations in winter respiratory activity under both daylight and dark conditions in assemblages dominated by *E. elongata*, with significantly higher respiration during the afternoon and first part of the night. Such diurnal variations are reflected by our findings, with maximal daytime respiration decreasing to lower levels across night-time emersion. Our data further demonstrated that seasonality in respiration was better reflected by night-time incubations, whereas no seasonal patterns were apparent in daytime rates. This is likely due to the influence of residual biological

446 activity after passage from light to dark conditions, given differences in the photo-
447 history of day and night incubated *C. officinalis*. Daytime samples were collected from
448 100% ambient irradiance and immediately transferred to complete darkness, whereas
449 night-time samples had been in darkness for a number of hours prior to incubations.
450 Future assessments may benefit from use of, for example, the Kok method for
451 determination of light respiration rates, as applied by Zou et al. (2011) to several
452 macroalgal species.
453
454 Differences between light and dark respiration rates have direct consequences for the
455 conventional calculation of gross production (*GP* = net production + respiration)
456 (Bensoussan and Gattuso, 2007), although estimates can be made for *C. officinalis*
457 using our data. Net production recorded at the start of tidal emersion ranged seasonally
458 from ca. 11 (December) to 26 (July) μmol DIC gDW^{-1} h^{-1}. Assuming our lower,
459 seasonally variable night-time rates of respiration to be representative, *C. officinalis GP*
460 is estimated as ranging 15.9 (March) to 27.7 (July) μmol DIC gDW^{-1} h^{-1}; though
461 December data are omitted due to the absence of night-time incubations. Similarly,
462 correcting net production with daytime respiration rates reveals a *GP* range of 16.7
463 (December) to 27.8 (July) μmol DIC gDW^{-1} h^{-1} for *C. officinalis*. These estimates are
464 highly comparable to *GP* reported for *E. elongata* from NW France during winter (11.8
465 ± 1.6 μmol C gDW^{-1} h^{-1}) and summer (22.5 ± 1.9 μmol C gDW^{-1} h^{-1}) (Egilsdottir et al.,
466 2015), and serve to highlight the high productivity of geniculate corallines in
467 comparison to other calcified algal groups. For example, Martin et al. (2006) reported
468 a seasonal range of 0.68 to 1.48 μmol C gDW^{-1} h^{-1} for the maerl forming *Lithothamnion*
469 *coralloides* off NW France. Currently, the contribution of coralline algae to global
470 carbon cycles is not well constrained, particularly that of geniculate turfing species (El

Haïkali et al., 2004; Van der Heijden and Kamenos, 2015). Given their comparatively high production identified here, our data indicate that geniculate corallines likely play a significant role in coastal carbon cycling, despite their presumably reduced overall benthic coverage as compared to maerl-forming or crustose coralline algal species. Inclusion of geniculate corallines into future estimates of coastal carbon cycles is therefore essential.

Over tidal emersion periods, patterns in *C. officinalis* production demonstrate the inorganic carbon (*Ci*) acquisition ability of this calcified alga over a range of CO_2 and HCO_3^- concentrations, however findings indicate potential vulnerability to periods of low irradiance e.g. winter. Maintenance of net production over July and September daytime tidal emersion, despite decreases in rock pool pCO_2 of 84% and 39%, respectively, highlight the ability of *C. officinalis* to effectively utilize both CO_2 and HCO_3^- as substrates for photosynthesis, as previously noted (Cornwall et al., 2012). This allows access to the relatively high HCO_3^- concentrations in seawater when CO_2 diffusion is limiting (Koch et al., 2013). During December and March, however, when overall minimal irradiance prevailed, a decrease in *C. officinalis* net production was observed. Estimation of *GP/R* ratios for these emersion periods (using daytime respiration data) revealed decreases from 3.45 to 1.9 over December-, and 3.93 to 1.2 over March- daytime emersion. Thus decreases in net production were driven by decreases in photosynthesis relative to respiration, which approached unity by the end of emersion in winter months. This reflects ecosystem wide *GP/R* ratios for assemblages dominated by *E. elongata* in the NW Mediterranean, which remained close to 1 (1.1 ± 0.1) over 24 h periods during winter (Bensoussan and Gattuso, 2007). Although neither water temperature, nor irradiance, showed significant change over

December or March tidal emersion, reductions in photosynthesis may have been driven by inorganic carbon limitation due to seasonal minima in irradiance. Under low light conditions, the ability to utilize HCO_3^- can be energetically limited, increasing reliance on CO_2 diffusion (Koch et al., 2013). *C. officinalis* photosynthesis may thus have been sensitive to the relatively small decrease in rock pool pCO_2 (ca. 30%) that occurred over December and March emersion periods.

4.2. Calcification

This study demonstrates that *C. officinalis* calcification is highly influenced by seasonal and diurnal variability in other metabolic processes (photosynthesis and respiration), in addition to the external carbonate chemistry environment. Across the entire annual cycle, *C. officinalis* calcification was highly predictable ($R^2 = 0.80$) by irradiance, water temperature and carbonate chemistry, providing a calculated NG_{max} of 3.94 µmol $CaCO_3$ gDW^{-1} h^{-1} and an E_k of 113.45 µmol photons m^{-2} s^{-1}. Irradiance was the greatest predictor of calcification (accounting for 76% of variability), reflecting photosynthetic enhancement of $CaCO_3$ precipitation (see below), although by contrasting light and dark calcification dynamics, the variable influences of physiology and external environment have been determined.

Light-enhanced calcification, i.e. $CaCO_3$ precipitation, was observed across the entire seasonal cycle, with maximal light-calcification rates during July and September in comparison to December and March. The seasonal range of net light-calcification was significantly higher than reported for the maerl species *L. corallioides* (Martin et al., 2006), comparable to *E. elongata* from NW France (Egilsdottir et al., 2015), and lower than reported for *E. elongata* from the Mediterranean (El Haïkali et al., 2004). Light-

enhanced calcification is typical for calcifying macroalgae, and is a product of light-dependent increase in carbonate saturation (ΩCO_3^{2-}) at the sites of calcification, due to photosynthetic activity (Littler, 1976; Koch et al., 2013). In the Corallinales, calcification takes place in the cell wall, from which CO_2 (and potentially HCO_3^-) uptake by adjacent cells for photosynthesis increases the pH, shifting the carbonate equilibrium in favour of ΩCO_3^{2-} and $CaCO_3$ precipitation (Littler, 1976; Borowitzka, 1982; Koch et al., 2013). Photosynthetic enhancement of *C. officinalis* calcification during the present study is strongly supported by the significant relationship identified between the two processes ($R^2 = 0.65$), as was also observed by Pentecost (1978). Interestingly, our data further demonstrated that internal enhancement of ΩCO_3^{2-} at the site of calcification, as opposed to external ΩCO_3^{2-}, was the dominant control on light-calcification rates. This was evidenced by a lack of increase in light calcification rates over summer tidal emersion periods, despite significant increases in rock pool pH and ΩCO_3^{2-}. With decreases in net production over daytime tidal emersion, e.g. during March, minimal levels of production were sufficient to maintain increased internal ΩCO_3^{2-}, permitting maintenance of calcification. This is supported by the overall lower E_k determined for calcification (ca. 110 µmol photons m^{-2} s^{-1}) as compared to net production (ca. 300 µmol photons m^{-2} s^{-1}).

In contrast to light calcification, the direction of *C. officinalis* dark calcification (dissolution vs. precipitation) was strongly related to rock pool water ΩCO_3^{2-}, mimicking abiotic $CaCO_3$ precipitation dynamics (Millero, 2007; Ries 2009). During seasonal minima of ΩCO_3^{2-}, net dissolution of $CaCO_3$ was apparent across dark daytime (December) and night-time (March) incubations, as observed during winter for *E. elongata* (Egilsdottir et al., 2015). With increases in pH and ΩCO_3^{2-} over March, July

and September daytime tidal emersion, initially negative (indicating net dissolution) or low positive dark calcification rates increased significantly, indicating net $CaCO_3$ precipitation at levels 40 – 46 % of light calcification. Additionally, net $CaCO_3$ precipitation was recorded across all dark daytime and night-time incubations during July, coinciding with seasonal maxima in ΩCO_3^{2-}. $CaCO_3$ precipitation in the dark has previously been documented for calcifying macroalgae (e.g. Pentecost, 1978; Borowitzka, 1981; Gao et al., 1993; Lee and Carpenter, 2001; de Beer and Larkum, 2001; Martin et al., 2006), typically at lower rates (e.g. 10 – 40 %) than light calcification (Pentecost, 1978; Borowitzka, 1981), and has been attributed to belated biological activity after a passage from light to dark conditions (Pentecost, 1978; Martin et al., 2006). Our findings demonstrate that dark calcification is possible over complete diurnal cycles for *C. officinalis*, and can be significantly exaggerated under conditions of rock pool water CO_3^{2-}-super-saturation. This mechanism can, however, be overridden by enhanced respiration. At the level of the organism, respiration can promote $CaCO_3$ dissolution via internal generation of CO_2 (Koch et al., 2013). During September, when maximal night-time respiration was observed, net $CaCO_3$ dissolution was apparent over the duration of night-time emersion, despite seasonal highs in ΩCO_3^{2-}. Dissolution pressures can thus be exacerbated by high rates of respiration, mitigating the positive impacts of maxima in external ΩCO_3^{2-}. This may have significant ramifications for the future fate of coralline algae if increases in water temperature drive corresponding increases in respiration.

Conclusions

Our findings indicate that *Corallina* species are highly tolerant to environmental stress, and are well-adapted to intertidal habitats, in agreement with previous studies

(Williamson et al., 2014; Guenther and Martone, 2014). Photosynthesis, respiration and calcification varied significantly with abiotic stressors, and strongly interacted with one another to produce predominantly beneficial outcomes at the level of the organism. With predicted acidification and warming of the world's oceans, the balance between these processes and the external environment may be perturbed. Whilst acidification may relieve putative CO_2 limitation in rock pools during low irradiance winter months, increases in night-time dissolution are predicted given the strong coupling between carbonate chemistry and dark calcification dynamics identified here. Similarly, whilst increasing temperatures may facilitate increases in gross productivity, temperature driven increases in night-time respiration could further exacerbate dark dissolution by reducing carbonate saturation at the sites of calcification. *Corallina officinalis* will be most vulnerable to future change during winter months, and monitoring to assess impacts should be focused on such periods. This study adds to the growing understanding of coralline algal physiology, and provides a baseline against which to monitor future change.

Acknowledgements

This work was funded by the NERC grant (NE/H025677/1).

References

Bensoussasn, N. and Gattuso, J-P.: Community primary production and calcification in a NW Mediterranean ecosystem dominated by calcareous macroalgae, Mar. Ecol. Prog. Ser., 334, 37–45, 2007.

Borowitzka, M.A.: Photosynthesis and calcification in the articulated coralline red algae *Amphiroa anceps* and *A. foliacea*, Mar. Biol., 62, 17–23, 1981.

Borowitzka, M.A.: Morphological and cytological aspects of algal calcification, Int. Rev. Cytol. Surv. Cell Biol., 74, 127–162, 1982.

Breeman, A.M.: Relative importance of temperature and other factors in determining geographic boundaries of seaweeds - experimental and phenological evidence. Helgolander Meeresuntersuchungen 42:199–241, 1988.

Brodie, J., Williamson, C., Barker, G.L., Walker, R.H., Briscoe, A., and Yallop, M.: Characterising the microbiome of *Corallina officinalis*, a dominant calcified intertidal red alga, FEMS Micro. Ecol., 92(8), doi: 10.1093/femsec/fiw110, 2016.

Brodie. J., Williamson, C.J., Smale, D.A. et al.: The future of the north-east Atlantic benthic flora in a high CO_2 world, Ecology and Evolution, 4(13), 2787–2798, 2014.

Cabello-Pasini, A. and Alberte, R.S.: Seasonal patterns of photosynthesis and light-independent carbon fixation in marine macrophytes, J. Phycol., 33, 321–329, 1997.

Chisholm, J.R.M. and Gattuso, J.P.: Validation of the alkalinity anomaly technique for investigating calcification and photosynthesis in coral-reef communities, Limnol. Oceanogr., 36, 1232–1239, 1991.

Cornwall, C.E., Hepburn, C.D., Pritchard, D., Currie, K.I., McGraw, C.M., Hunter, K.A. and Hurd, C.L.: Carbon-use strategies in macroalgae: differential responses to lowered pH and implications for ocean acidification, J. Phycol., 48, 137–144, 2012.

Coull, B.C. and Wells, J.B.J.: Refuges from fish predation - experiments with phytal meiofauna from the New Zealand rocky intertidal, Ecology, 64, 1599–1609, 1983.

De Beer, D. and Larkum, A.W.D.: Photosynthesis and calcification in the calcifying algae *Halimeda discoidea* studied with microsensors, Plant Cell Environ., 24, 1209–1217, 2001.

Dickson, A.G. and Millero, F.J: A comparison of the equilibrium constants for the dissociation of carbonic acid in seawater media. Deep Sea Res. Part A Oceanogr. Res. Pap., 34, 1733–1743, 1987.

Egilsdottir, H., Olafsson, J. and Martin, S.: Photosynthesis and calcification in the articulated coralline alga *Ellisolandia elongata* (Corallinales, Rhodophyta) from intertidal rock pools, Eur. J. Phycol., 51(1), 59–70, 2015.

Egilsdottir, H., Noisette, F., Noël, L.M-L.J., Olafsson, J. and Martin, S.: Effects of pCO_2 on physiology and skeletal mineralogy in a tidal pool coralline alga *Corallina elongate*, Mar. Biol., 160, 2103–2112, 2013.

El Haïkali, B., Bensoussan, N., Romano, J. and Bousquet, V.: Estimation of photosynthesis and calcification rates of *Corallina elongata* Ellis and Solander ,1786, by measurements of dissolved oxygen, pH and total alkalinity, Sci. Mar., 68, 45–56, 2004.

Ganning, B.: Studies on chemical, physical and biological conditions in Swedish rockpool ecosystems, Ophelia, 9, 51–105, 1971.

Gao, K., Aruga, Y., Asada, K., Ishihara, T., Akano, T. and Kiyohara, M.: Calcification in the articulated coralline alga *Corallina pilulifera*, with special reference to the effect of elevated CO_2 concentration, Mar. Biol., 117, 129–132, 1993.

Grömping, U.: Relative Importance for linear regression in R: The Package relaimpo, J. Stat. Softw., 17, 1–27, 2006.

Guenther, R.J. and Martone, P.T.: Physiological performance of intertidal coralline algae during a simulated tidal cycle, J. Phycol., 50, 310–321, 2014.

Hofmann, L. and Bischof, K.: Ocean acidification effects on calcifying macroalgae, Aquat. Biol., 22, 261–279, 2014.

Hofmann, L., Straub, S. and Bischof, K.: Competition between calcifying and noncalcifying temperate marine macroalgae under elevated CO_2 levels, Mar. Ecol. Prog. Ser., 464, 89–105, 2012a.

Hofmann, L., Yildiz, G., Hanelt, D. and Bischof, K.: Physiological responses of the calcifying rhodophyte, *Corallina officinalis* (L.), to future CO_2 levels, Mar. Biol. 159, 783–792, 2012b.

Israel, A. and Hophy, M.: Growth, photosynthetic properties and Rubisco activities and amounts of marine macroalgae grown under current and elevated seawater CO_2 concentrations. Glob Chang Biol 8:831–840, 2002.

Johansen, H.W.: Coralline Algae: A first synthesis. CRC Press, Boca Raton, Florida, USA. p239, 1981.

Johnston, A.M., Maberly, S.C. and Raven, J.A.: The acquisition of inorganic carbon by four red macroalgae. Oecologia 92:317–326, 1992.

Jones, C.G., Lawton, J.H. and Shachak, M.: Organisms as ecosystem engineers, Oikos, 69, 373–386, 1994.

Jokiel, P.L.: Ocean acidification and control of reef coral calcification by boundary layer limitation of proton flux. Bull Mar Sci 87:639–657, 2011.

Jueterbock, A., Tyberghein, L., Verbruggen, H., Coyer, J.A., Olsen, J.L. and Hoarau, G.: Climate change impact on seaweed meadow distribution in the North Atlantic rocky intertidal. Ecol Evol 3:1356–73, 2013.

Kanwisher, J.: Photosynthesis and respiration in some seaweeds. In: Barnes H (ed) *Some Contemporary Studies in Marine Science.* George Allen and Unwin LTD, London. pp407–420, 1966.

Kelaher, B.P.: Influence of physical characteristics of coralline turf on associated macrofaunal assemblages, Mar. Ecol. Prog. Ser., 232, 141–148, 2002.

Kelaher, B.P.: Changes in habitat complexity negatively affect diverse gastropod assemblages in coralline algal turf, Oecologia, 135, 431–441, 2003.

Koch, M., Bowes, G., Ross, C. and Zhang, X-H.: Climate change and ocean acidification effects on seagrasses and marine macroalgae, Glob. Chang. Biol., 19, 103–32, 2013.

Lee, D. and Carpenter, S.J.: Isotopic disequilibrium in marine calcareous algae, Chem. Geol., 172, 307–329, 2001.

Littler, M.: Calcification and its role among the macroalgae, Micronesica, 12(1), 27–41, 1976.

Littler, M., Littler, D.S., Blair, S.M. and Norris, J.N.: Deepest known plant life discovered on an uncharted seamount, Science, 227, 57–59, 1985.

Lüning, K.: Seaweeds: their environment, biogeography and ecophysiology, John Wiley & Sons, New York, NY, USA, 1990.

Martin, S., Castets, M.D. and Clavier, J.: Primary production, respiration and calcification of the temperate free-living coralline alga *Lithothamnion corallioides*, Aquat. Bot., 85, 121–128, 2006.

Martin, S., Clavier, J., Chauvaud, L. and Thouzeau, G.: Community metabolism in temperate maerl beds. I. Carbon and carbonate fluxes, Mar. Ecol. Prog. Ser., 335, 19–29, 2007.

Martin, S. and Gattuso, J-P.: Response of Mediterranean coralline algae to ocean acidification and elevated temperature, Glob. Chang. Biol., 15, 2089–2100, 2009.

Maberly, S.C.: Exogenous sources of inorganic carbon for photosynthesis by marine macroalgae. J Phycol 26:439–449, 1990.

McCoy, S. and Kamenos, N.A.: Coralline algae (Rhodophyta) in a changing world: integrating ecological, physiological, and geochemical responses to global change, J. Phycol., DOI: 10.1111/jpy.12262, 2015.

Mehrbach, C., Culberson, C.H., Hawley, J.E. and Pytkowicz, R.M.: Measurement of the apparent dissociation constants of carbonic acid in seawater at atmospheric pressure, Limnol. Oceanogr., 18, 897–907, 1973.

Millero, F.J.: The marine inorganic carbon cycle, Chem. Rev., 107, 308–341, 2007.

Morris, S. and Taylor, A.C.: Diurnal and seasonal-variation in physicochemical conditions within intertidal rock pools, Estuar. Coast Shelf Sci., 17, 339–355, 1983.

Nelson, W.A.: Calcified macroalgae - critical to coastal ecosystems and vulnerable to change: a review, Mar. Freshw. Res., 60, 787, 2009.

Perkins, R.G., Williamson, C.J., Brodie, J., Barille, L., Launeau, P., Lavaud, J., Yallop, M.L. and Jesus, B.: Microspatial variability in community structure and photophysiology of calcified macroalgal microbiomes revealed by coupling of

hyperspectral and high-resolution fluorescence imaging, Scientific Reports, 6, 22343, 2016.

Pentecost, A.: Calcification and photosynthesis in *Corallina officinalis* L. using CO_2 C-14 method, Br. Phycol. J., 13, 383–390, 1978.

Pierrot, D., Lewis, E. and Wallace, D.W.R.: MS Excel program developed for CO2 system calculations, Tech. rep., Carbon Dioxide Inf. Anal. Cent., Oak Ridge Natl. Lab, US DOE, Oak Ridge, Tennessee, 2016.

R Core Team: R: A Language and Environment for Statistical Computing, 2014.

Ries, J.B.: Effects of secular variation in seawater Mg/Ca ratio (calcite-aragonite seas) on $CaCO_3$ sediment production by the calcareous algae *Halimeda*, *Penicillus* and *Udotea* - evidence from recent experiments and the geological record, Terra. Nov., 21, 323–339, 2009.

Ries, J.B.: A physicochemical framework for interpreting the biological calcification response to CO2-induced ocean acidification. Geochim. Cosmochim. Acta. 75:4053–4064, 2011.

Smith, S. and Key, G.: Carbon dioxide and metabolism in marine environments, Limnol. Oceanogr., 20, 493–495, 1975.

Van der Heijden, L.H. and Kamenos, N.A.: Calculating the global contribution of coralline algae to total carbon burial, Biogeosciences, 12, 6429–6441, 2015.

Venables, W.N. and Ripley, B.D.: Modern Applied Statistics with S, Fourth. Springer, New York, 2002.

Williamson, C.J., Brodie, J., Goss, B., Yallop, M., Lee, S. and Perkins, R.: *Corallina* and *Ellisolandia* (Corallinales, Rhodophyta) photophysiology over daylight tidal emersion: interactions with irradiance, temperature and carbonate chemistry, Mar. Biol., 161, 2051–2068, 2014a.

Williamson, C.J., Najorka, J., Perkins, R., Yallop, M.L. and Brodie, J.: Skeletal mineralogy of geniculate corallines: providing context for climate change and ocean acidification research, Mar. Ecol. Prog. Ser., 513, 71–84, 2014b.

Williamson, C.J., Walker, R.H., Robba, L., Russell, S., Irvine, L.M. and Brodie, J.: Towards resolution of species diversity and distribution in the calcified red algal genera *Corallina* and *Ellisolandia* (Corallinales, Rhodophyta), Phycologia, 54(1), 2–11, 2015.

Zou, D., Kunshan, G.A.O. and Jianrong, X.I.A.: Dark respiration in the light and in darkness of three marine macroalgal species grown under ambient and elevated CO_2 concentrations, Acta. Oceanol. Sin., 30(1), 106–112, 2011.

Figures

Figure 1. Sampling site and habitat, showing location of Combe Martin (a), and an example upper-shore rock pool (b) dominated by turfing assemblages of *Corallina officinalis* (c).

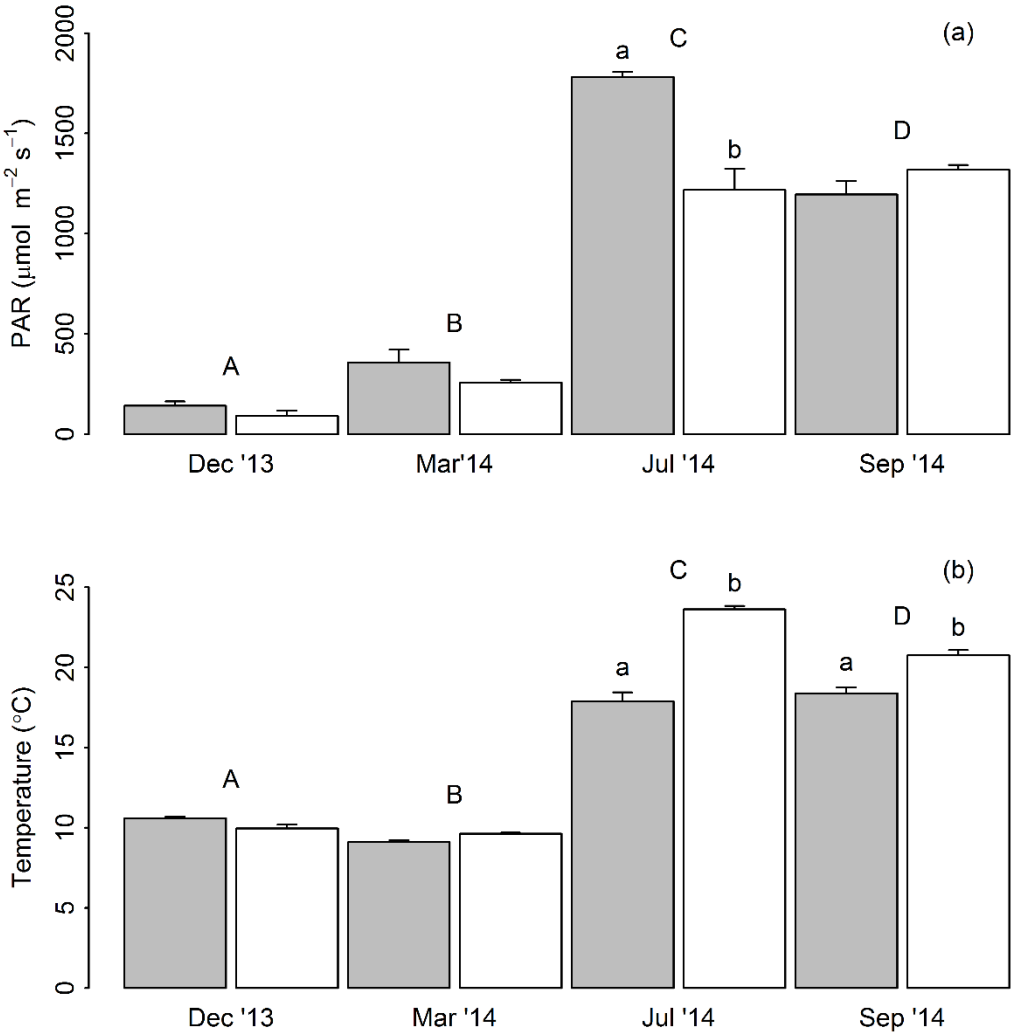

805

806 **Figure 2:** Irradiance (a) and rock pool water temperature (b) recorded at the start (grey
807 bars) and end (white bars) of daytime tidal emersion periods during December 2013
808 (Dec ’13), and March (Mar ’14), July (Jul’14) and September (Sep ’14) 2014 (Average
809 ± SE). Upper-case and lower-case letters denote TukeyHSD homogenous subsets in
810 relation to the factors ‘month’ and ‘tide’, respectively.

811

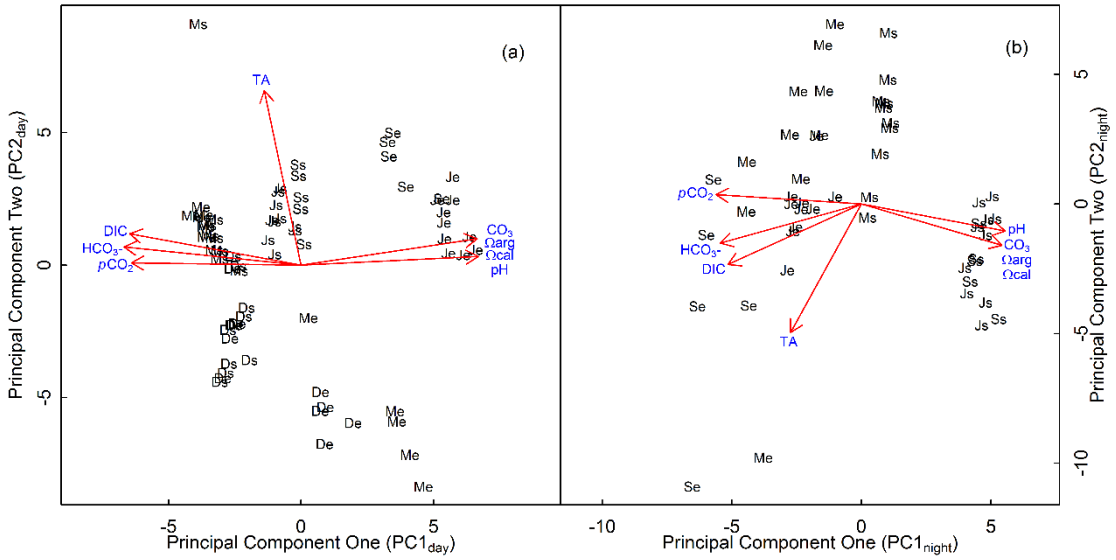

Figure 3: Principal components analysis of (a) daytime and (b) night-time carbonate chemistry parameters, showing principal component one in relation to principal component two. Upper-case letters indicate sampling month (D = December, M = March, J = July, S = September) and lower-case letters indicate start (s) or end (e) tidal emersion.

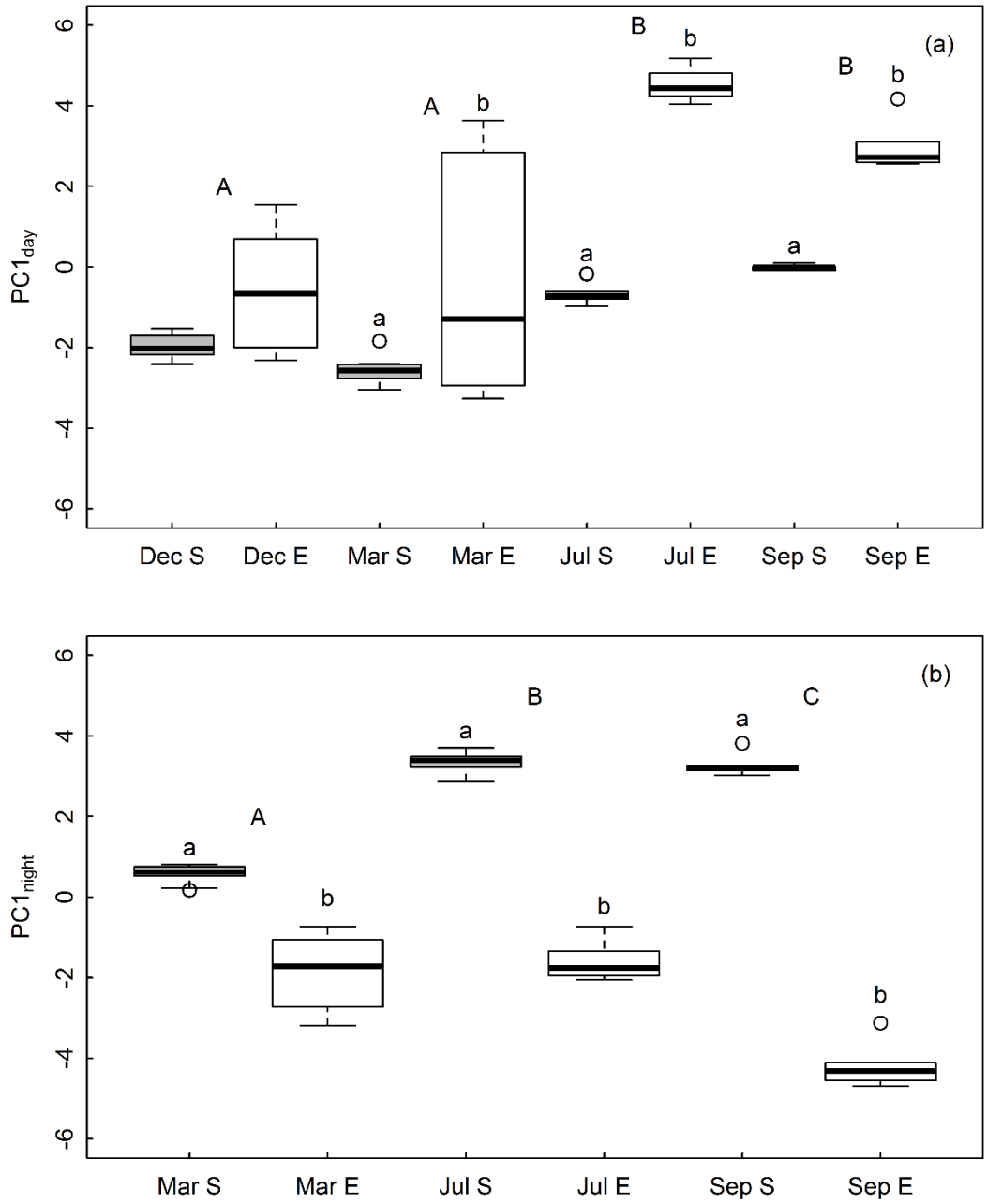

819

820 **Figure 4:** Boxplots showing the median, minimum, maximum and first and third
821 quartiles of $PC1_{day}$ (a) and $PC1_{night}$ (b) in relation to sampling month (Dec = December,
822 Mar = March, Jul = July, Sep = September) and tidal emersion period (S = start, E =
823 End). Upper-case and lower-case letters denote TukeyHSD homogenous subsets in
824 relation to the factors 'month' and 'tide', respectively.

825

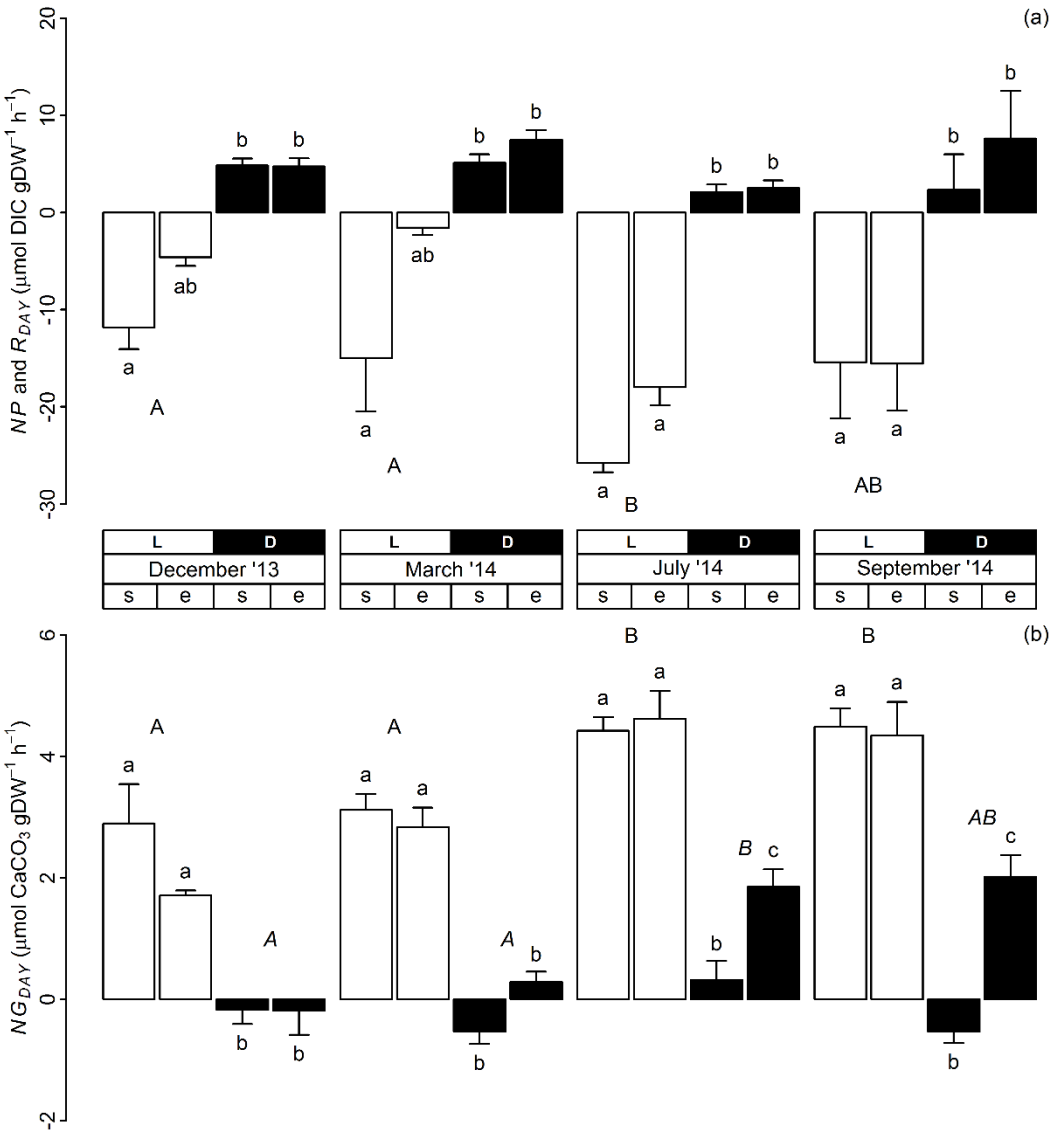

826

827 **Figure 5:** Average daytime (a) *NP* (-ve DIC flux) and R_{DAY} (+ve DIC flux), and (b)
828 NG_{DAY} as determined from light (L – white bars) and dark (D – black bars) treatment
829 incubations conducted at the start (s) and end (e) of daytime tidal emersion periods
830 during December 2013 and March, July and September 2014 (Average ± SE, n = 5).
831 Upper-case and lower-case letters denote TukeyHSD homogenous subsets in relation
832 to the factors 'month' and 'tide', respectively.

833

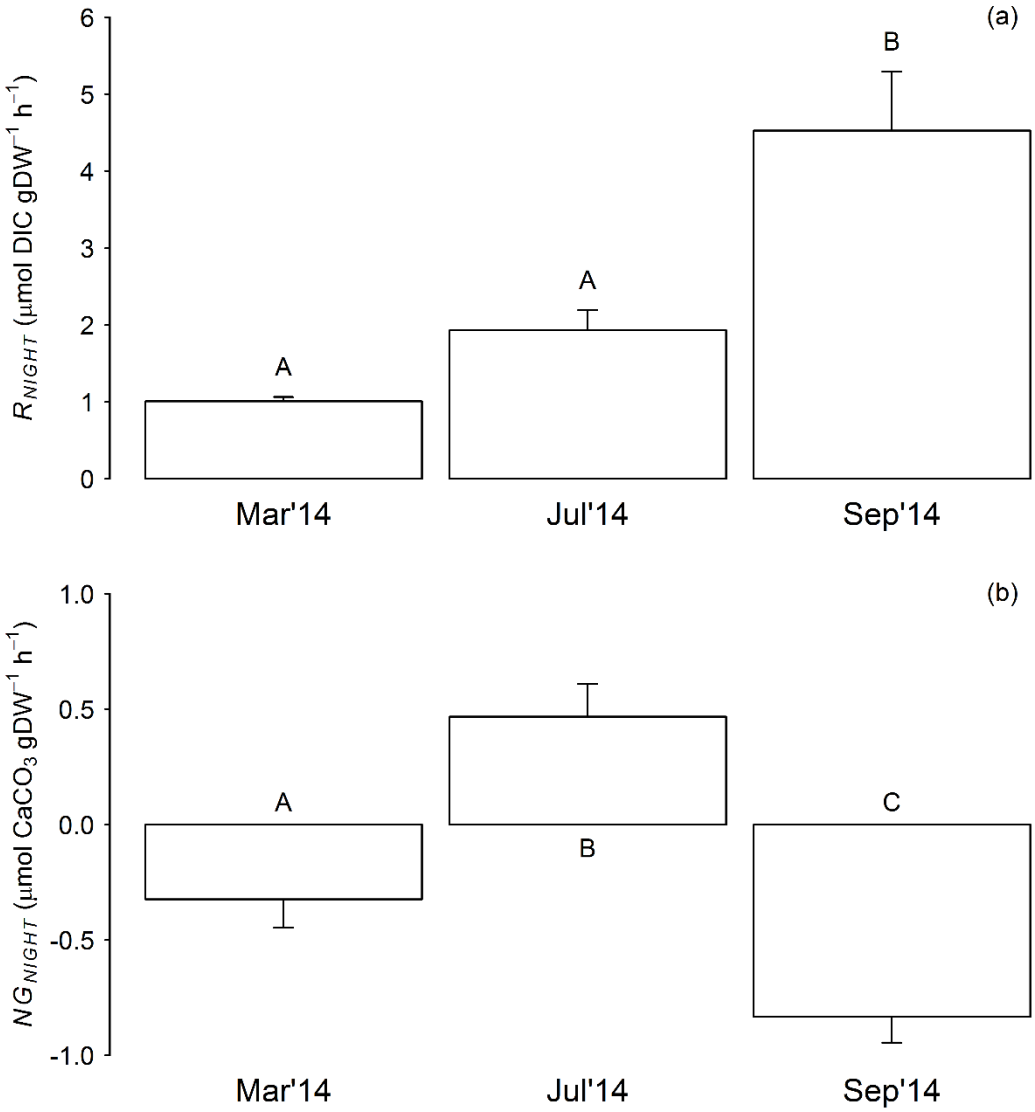

834
835 **Figure 6:** Average night-time (a) R_{NIGHT} and (b) NG_{NIGHT} as determined across both
836 light/dark treatment incubations and the start/end of tidal emersion periods (Average
837 ± SE, n = 20). Upper-case letters denote TukeyHSD homogenous subsets in relation
838 to the factor 'month'.
839

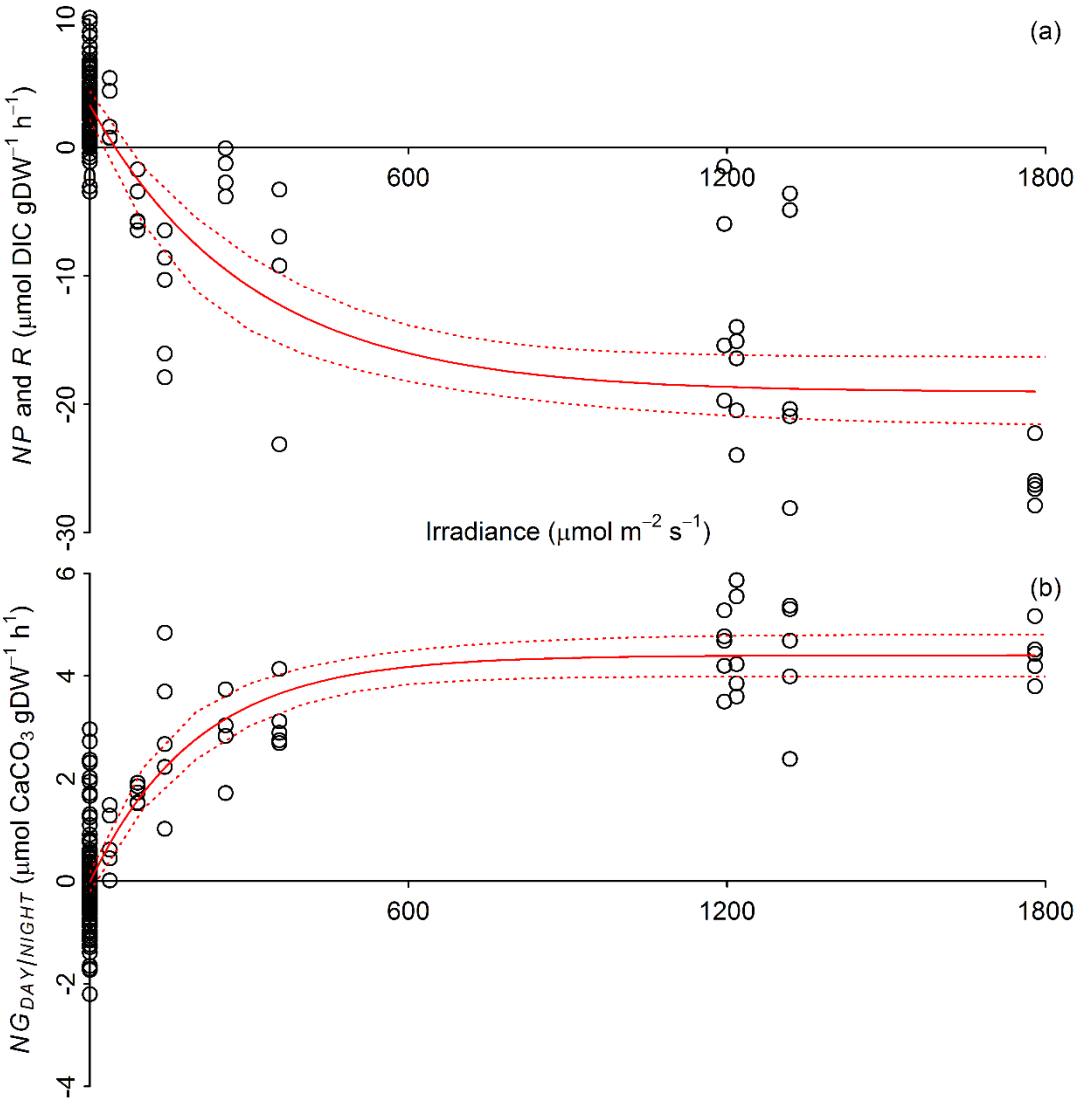

840

841 **Figure 7:** Relationship of (a) net production/respiration (*NP* and *R*) and (b) net
842 calcification ($NG_{DAY/NIGHT}$) to the average irradiance measured during respective
843 incubations (Model 1, Table 4), showing regression line (solid red line) and 95 %
844 confidence intervals (dashed red lines).

845
846

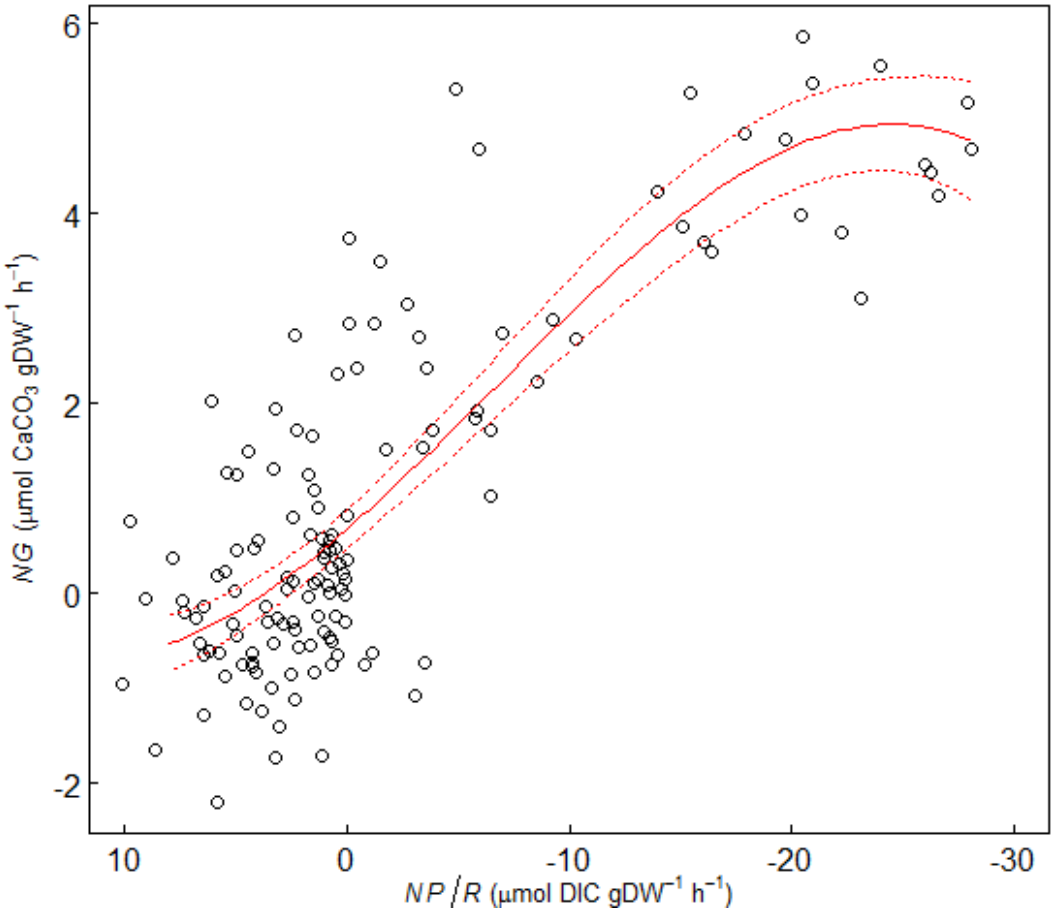

Figure 8: Relationship between calcification (*NG*) and production / respiration (*NP/R*), showing regression line (solid red line) and 95 % confidence intervals (dashed red lines).

863 **Tables**

864

865 **Table 1:** Sampling dates and tidal details. Experimental rock pools were located at
866 5.5 m relative to chart datum. All times are expressed in GMT.

Sampling Date							
Dec 4th/5th 2013		Mar 16th/17th 2014		Jul 1st/2nd 2014		Sep 9th/10th 2014	
Time	Height (m)	Time	Height (m)	Time	Height (m)	Time	Height (m)
06:30	9.6	05:50	8.8	08:12	8.4	05:46	9.7
12:30	0.7	11:51	1.2	13:59	1.6	11:50	0.4
18:50	9.5	18:09	8.9	20:23	8.5	18:08	10.1
00:55	0.8	00:02	1	02:20	1.7	00:13	0.2
07:15	9.7	06:23	9	08:45	8.2	06:31	9.9

867

868

869 **Table 2**: Component loadings of principal components analysis of daytime and night-
870 time carbonate chemistry parameters (TA, DIC, pH, pCO_2, HCO_3^-, CO_3^{2-}, Ω_{arg} and Ω_{cal})

871

	$PC1_{DAY}$ (%)	$PC2_{DAY}$ (%)	$PC1_{NIGHT}$ (%)	$PC2_{NIGHT}$ (%)
Proportion of variance	84.3	13.2	83.6	16.0
Cumulative proportion	84.3	97.6	83.6	99.7
Variable	$PC1_{DAY}$	$PC2_{DAY}$	$PC1_{NIGHT}$	$PC2_{NIGHT}$
Component Loadings				
TA	-0.07	0.94	-0.18	-0.77
DIC	-0.36	0.17	-0.35	-0.36
pH	0.38	0.04	0.37	-0.16
pCO_2	-0.36	0.01	-0.38	0.05
HCO_3^-	-0.38	0.09	-0.37	-0.23
CO_3^{2-}	0.37	0.14	0.37	-0.24
Ω_{arg}	0.37	0.14	0.37	-0.24
Ω_{cal}	0.37	0.14	0.37	-0.24

872

Table 3: Multiple linear regression analysis of $PC1_{DAY}$ in relation to irradiance (Irrad.) or cumulative photodose (Photo.) plus water temperature (Temp.), and linear regression analysis of $PC1_{NIGHT}$ in relation to water temperature (Temp.), showing associated standard error (*SE*) of coefficients, the significance of predictor variables (Pred. sig.) within the model, the percent relative importance of predictor variables (Rel. Imp.), the proportion of variance explained by the regression (R^2), the overall model significance (*P*), and the number of observations (*n*).

Relationship ($y = a + b_1*X_1 + b_2*X_2$)	Coefficient *SE*			Pred. sig.		Rel.Imp. (%)		R^2	*P*	*n*
	a	b_1	b_2	X_1	X_2	X_1	X_2			
$PC1_{DAY}$ = -7.03 + -0.002*Irrad. + 0.61*Temp.	0.73	0.00	0.07	<0.001	<0.001	28	71	0.63	<0.001	96
$PC1_{DAY}$ = -2.52 + 1.41^{-7}*Photo. + 9.10^{-2}*Temp.	0.72	2.72^{-8}	6.38^{-2}	<0.001	<0.01	58	41	0.69	<0.001	96
$PC1_{NIGHT}$ = -2.89 + 0.22*Temp.	1.40	0.10	-	<0.05	<0.05	-	-	0.08	<0.05	72

Table 4: Values of parameters (*SE* in parentheses) calculated by non-linear regression of net production (*NP*, μmol DIC gDW^{-1} h^{-1}) and net calcification (*NG*, μmol $CaCO_3$ gDW^{-1} h^{-1}): in relation to (Model 1) irradiance (*E*, μmol photons m^{-2} s^{-1}), where c is estimated dark respiration or calcification; and in relation to (Model 2) irradiance and temperature (*T*, ^{o}C), where f is a constant; and in relation to (Model 3) irradiance and carbonate chemistry (*PC1*); and in relation to (Model 4) irradiance, temperature and carbonate chemistry. Asterisks denote coefficient significance in models (*P* <0.05*, *P* <0.01**, *P* <0.001***). Estimation of overall model fit is presented as the proportion of variance explained by the regression (R^2) and as Akaike Information Criterion (*AIC*). *n* denotes the number of observations.

	$P(G)_{max}$	*Ek*	*c*	*d*	*e*	*f*	R^2	*AIC*	*n*
Model 1: $NP\ (NG) = P(G)_{max}\ (1\text{-}e^{-E/Ek}) + c$									
NP	-22.3(1.48)***	300(65)***	3.29(0.56)***				0.67	885	140
NG	4.41(0.22)***	200(34)***	-0.01(0.09)**				0.76	383	140
Model 2: $NP\ (NG) = P(G)_{max}\ (1\text{-}e^{-E/Ek}) + dT + f$									
NP	-23.8(1.97)***	377(99)***		0.15(0.12)		1.07(1.82)	0.68	886	140
NG	3.92(0.21)***	115(24)***		0.08(0.01)***		-1.28(0.26)***	0.80	363	140
Model 3: $NP\ (NG) = P(G)_{max}\ (1\text{-}e^{-E/Ek}) + ePC1 + f$									
NP	-23.0(1.62)***	343(80)***			0.29(0.20)	3.24(0.56)***	0.68	885	140
NG	4.18(0.21)***	149(27)***			0.13(0.03)***	-0.03(0.08)*	0.79	367	140
Model 4: $NP\ (NG) = P(G)_{max}\ (1\text{-}e^{-E/Ek}) + dT + ePC1 + f$									
NP	-23.6(1.96)***	375(99)***		0.07(0.14)	0.22(0.23)	2.12(2.12)	0.68	887	140
NG	3.94(0.20)***	113(23)***		0.06(0.02)**	0.08(0.03)*	-0.93(0.30)**	0.80	360	140